Extended Abstracts of the 2005 International Conference on Solid State Devices and Materials, Kobe, 2005, pp.684-685

P6-3

Origin of Frequency Dependence in Drain Conductance of InAlAs/InGaAs HEMTs

Hirohisa Taguchi, Maki Hayakawa, Yuki Nakamura, Tsutomu Iida, and Yoshifumi Takanashi

Department of Materials Science and Technology, Faculty of Industrial Science and Technology
Tokyo University of Science
2641 Yamazaki, Noda, Chiba Pref., 278-8510 Japan
Telephone +81 4 7124 1501 Ext. 4312, Facsimile +81 4 7123 9362 E-mail: ht0131@rs.noda.tus.ac.jp

1. Introduction

The drain conductance (G_d) of HEMTs composed of the InAlAs/InGaAs material system is frequency dependent, which is a serious concern with regard to their use in high frequency circuits such as wideband analog and digital ICs. The cause of this frequency dependence is not yet clear, although some reports have suggested that its origin is the surface states of the source region. Through a study of the effects of optical irradiation on HEMT characteristics, we have shown that the shift in the threshold voltage (V_{TH}) is caused by the change in the Fermi level due to an accumulation of holes in the source region [1, 2]. Our purpose in this paper is to show that the frequency dependence of HEMT G_d is caused by the same mechanism as the V_{TH} shift.

2. Results and discussion

The schematic structure of InAlAs/InGaAs HEMTs we used in this paper is shown in Fig. 1. The gate length and width of the HEMTs were 0.1 and 40 μm, respectively. The InGaAs channel layer was 15 nm thick. The barrier layer was InAlAs and the sheet density of the two-dimensional electron gas (2DEG) was 2 x 10^{12} cm^{-2}. Figure 2 shows the typical drain current-voltage characteristics of HEMT as measured at room temperature. Figure 3 shows the responsivity (Res) of HEMT measured using an HP8510B signal analyzer when the modulated light from a 1.3-μm-wavelength laser diode was irradiated onto the back-side of the wafer. The Res has a Lorentz-type frequency dependence, f_{3dB} being the 3-dB bandwidth [2]. Figure 4 shows the typical frequency dependence of G_d measured using an HP8702A signal analyzer. G_d was almost constant over the measured frequency range at a source-to-drain voltage (V_{ds}) less than 1 V, while its frequency dispersion appeared at a V_{ds} higher than 1.4 V.
The frequency dependence of Res arises from the recombination of 2DEG with holes accumulated at the source region and thus f_{3dB} is restricted by the minority carrier (hole) lifetime (τ) [1, 2]. According to the previous work [3], holes are generated at the drain region through the avalanche multiplication mechanism under a high electrical field and accumulate at the source region. If the origin of frequency dependence in G_d is due to the same mechanism as mentioned in Res, G_d can be understood by dividing it into two parts:

$$G_d(f) = G_{d0} + G_{d1}(f) \text{ and } G_{d1}(f) = G_{d10} \Big/ \sqrt{1+(f/f_{3dB})^2}, \quad (1)$$

where the second term G_{d1} (f) is related to the avalanche multiplication and expresses a Lorentz-type frequency dependence. The DC component of G_d is given by the sum of G_{d0} and G_{d10}. Figure 5 shows $G_{d1}(f)$, which we obtained by applying Eq. (1) to the G_d data of Fig. 4, as a function of frequency. The frequency dependence of Res was similar to that of $G_{d1}(f)$. Calculated f_{3dB} from the experimental results of Figs. 3 and 5 were 1.02x10^8 Hz and 1.23x10^8 Hz, respectively, and both values were almost same. This proves that the frequency dependence of G_d can also be explained by the same model as mentioned in Res. To confirm the validity of this physical model, we repeated the experiment described above at several drain-to-gate effective voltages, $V_{DG,eff}$. The results are shown in Fig. 6

To understand physically the experimental results described above, we estimated theoretically the energy state and carrier concentration for a system where both electrons and holes co-exist by taking yet clear account self-consistent solutions of both the Schrödinger and Poisson equations. In this calculation, the surface potential was assumed to be 0.6 V for convenience and ps is defined as the sheet concentration of holes accumulated at the source region. Figure 7 (a) shows the energy band diagram for the conduction band and the carrier concentration of 2DEG (p_s=0). Figure 7 (b) shows the energy band diagram for the conduction and valence bands and the carrier concentrations of 2DEG and 2DHG (two-dimensional hole gas) for p_s=1.06x10^{12} cm^{-2}. Due to the internal field, holes accumulate at the heterointerface on the side of the substrate. On the other hand, electrons distribute not only at the heterointerface on the side of the surface but at the heterointerface on the side of the substrate so as to maintain the charge neutrality. Figure 8 shows the minority carrier lifetime, τ_{Total}, calculated taking account of the carrier distribution as a function of p_s. In this figure, τ_{Br} means the radiative recombination lifetime and τ_{CHSH} Auger recombination lifetime for the CHSH process. When p_s exceeds 10^{12} cm^{-2}, τ_{Total} is dominated by the Auger recombination mechanism and decreases drastically with increasing p_s. In Fig. 6, τ was almost constant when V_{ds} was less than 1.4 V and then decreased when V_{ds} was more than 1.4 V. The reason for this is that ps generated through avalanche multiplication exceeds 10^{12} cm^{-2} when V_{ds} increases beyond 1.4 V. Figure 9 shows p_s as a function of $1/V_{DG,eff}$ at V_{gs} of 0 V, deduced from the results of Figs. 6 and 8. This result is very resemble to that of $1/V_{DG,eff}$ dependence of recombination-induced electroluminescence intensity at the source region reported by Shigekawa et al. [3]. Therefore, holes observed in our study are obviously generated by the avalanche multiplication because $V_{DG,eff}$ is proportion to the effective electric field at the drain.

The shift of V_{TH} (ΔV_{TH}) is correlated with p_s [2]. If

ΔV_{TH} is known as a function of V_{DS} via the relationship of V_{DS} to p_s (Fig. 9), an increase in the drain current (ΔI_{DS}) due to the avalanche multiplication can be estimated using the relation $\Delta I_{DS} = Gm\Delta V_{TH}$. Figure 10 shows the drain I-V characteristics at V_{GS}=0 V with and without the avalanche multiplication, where V_{TH} is different from that for Fig. 2 and Gm is assumed to be 70 mS. The latter result resembles I-V characteristics as usually observed in short gate FETs.

3. Conclusion

Our experimental and calculated results prove that the frequency dependence of G_d is caused by holes accumulated at the source region and their recombination with the 2DEG.

4. References

[1] Y. Takanashi et al., *IEEE EDL.*, vol.19, p.472, 1998.
[2] Y. Takanashi et al., *IEEE TED.*, vol.46, p.2271, 1999.
[3] N. Shigekawa et al., *IEEE TED.*, vol.44, p.513, 1997.

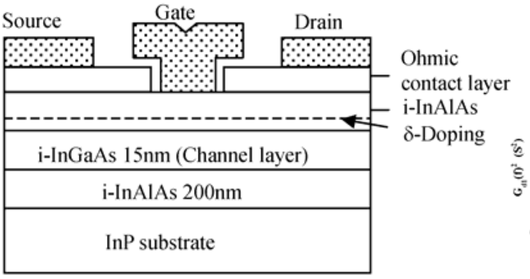

Fig. 1. Schematic cross sectional view of InAlAs/InGaAs HEMT.

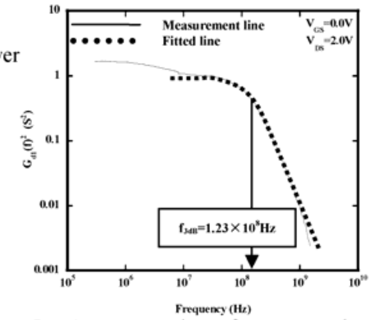

Fig. 5. An example of measured $G_{d1}(f)^2$ of HEMTs; The dashed line represents $G_{d1}(f)$ fitted using Eq. (1).

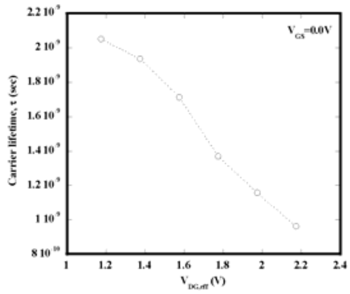

Fig. 6. Minority carrier (hole) lifetime τ as a function of $V_{DG,eff}$, which were estimated using the relation of $\tau=1/2\pi f_{3dB}$.

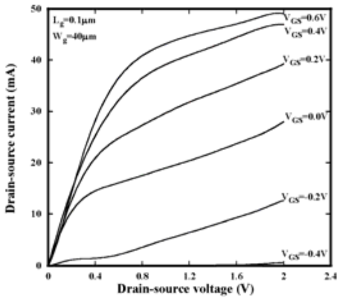

Fig. 2. Typical drain current-voltage characteristics of InAlAs/InGaAs HEMT.

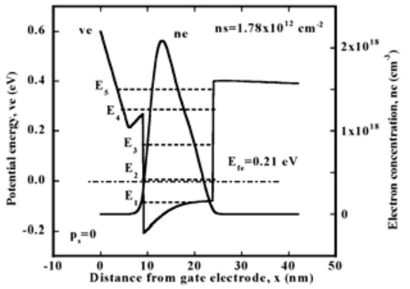

Fig. 7 (a)

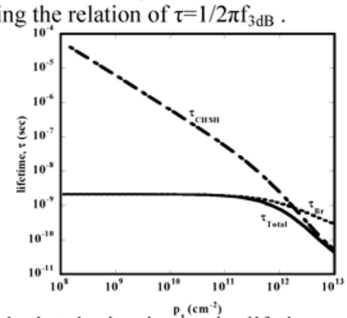

Fig. 8. Calculated minority carrier lifetime; τ_{Total} as p_s accumulated at the source region. τ_{Br} mean the radiative recombination time. τ_{CHSH} mean Auger recombination time for CHSH process.

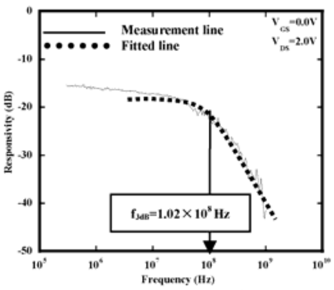

Fig. 3. An example of measured responsivity of HEMTs when irradiated with modulated light; The dashed line represents $G_{d1}(f)$ fitted using Eq. (1).

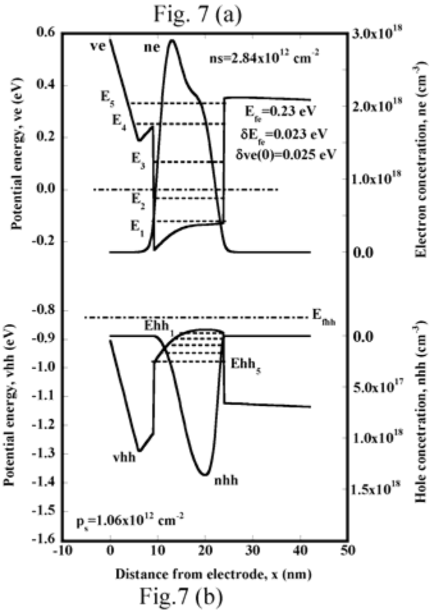

Fig.7 (b)

Fig. 7. The energy band diagram
(a) The energy band diagram for the conduction band and the carrier concentration of 2DEG (p_s=0).
(b) The energy band diagram for the conduction and valence bands and the carrier concentrations of 2DEG and 2DHG for p_s=1.06x10^{12} cm^{-2}.

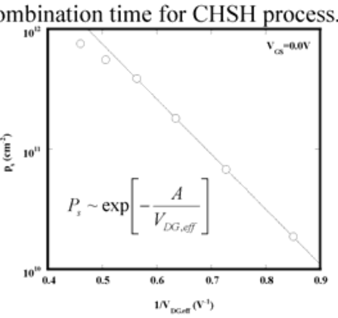

Fig. 9. p_s as a function of $1/V_{DG,eff}$ at V_{GS} of 0 V, deduced from the results of Figs. 6 and 8.

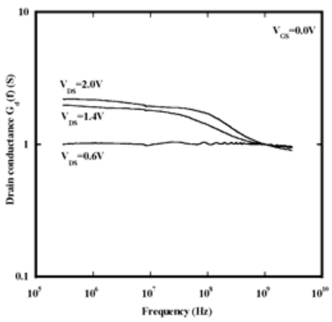

Fig. 4. Typical frequency dependence of G_d (f) of HEMT.

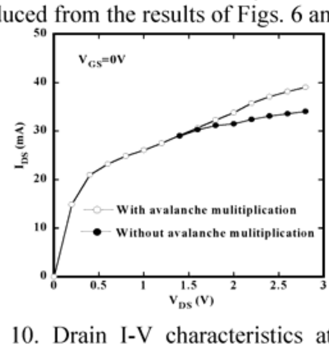

Fig. 10. Drain I-V characteristics at V_{GS}=0 V with and without the avalanche multiplication, where V_{TH} is different from that for Fig. 1 and Gm is assumed to be 70 mS.